KACST-FORUM

Dry reforming of methane over ZrO_2-supported Co–Mo carbide catalyst

X. Du · L. J. France · V. L. Kuznetsov ·
T. Xiao · P. P. Edwards · Hamid AlMegren ·
Abdulaziz Bagabas

Abstract The process of dry reforming of methane has the potential to be an effective route for CO_2 utilization via syn-gas production. In the present study, ZrO_2-supported Co–Mo bimetallic carbide catalysts were prepared via a co-precipitation method through a combined reduction and carburization procedure employing a CH_4/H_2 (20/80 %) mixture. All of the as-synthesized materials were tested at 850°, under atmospheric pressure and a CO_2:CH_4 ratio of 1. The importance of the ZrO_2 support became immediately apparent when it exhibited a higher conversion than the corresponding low-surface-area bulk Mo_2C catalyst, which we attribute to lewis acid and base active sites on the surface of ZrO_2. From catalytic tests and pre-and post-reaction X-ray diffraction (XRD) patterns, we observed that different dispersions of the monometallic carbides, caused by varying the pre-heating temperatures on ZrO_2, did not significantly affect conversion or yield. In contrast, incorporation of cobalt atoms into the Mo_2C lattice significantly enhanced the conversion, yield and stability of the catalysts. Post-reaction XRD patterns indicated that the bimetallic carbide had enhanced the resistance to the oxidation effect that is known to deactivate Mo_2C catalysts. In addition, increasing the Co loading in the mixed metal carbides was seen to enhance the resistance of the catalyst to the reverse water gas shift reaction, leading to improved stability of the H_2 yields.

Keywords Dry reforming of methane · Synthesis gas · Bimetallic carbide · Zirconia support

Introduction

The dry reforming of methane $(DRM, CO_2 + CH_4 \rightarrow 2CO + 2H_2, \Delta H^o_{298} = +247 \text{ KJmol}^{-1})$ is an effective method to utilize CO_2, via a reaction with CH_4 to produce a mixture of CO and H_2 known as "synthesis gas (syn-gas)" [2]. This reaction is, however, highly endothermic and generally high temperatures are required both for significant levels of conversion as well as for reducing side reactions. The DRM process provides several advantages over steam reforming of methane $(SRM, H_2O + CH_4 \rightarrow CO + 3H_2, \Delta H^o_{298} = +206 \text{ KJmol}^{-1})$, and perhaps the most important one is the production of syn-gas with a low H_2/CO ratio, which is suitable for use in forming higher level alcohols [10] (in a stoichiometric reaction, the H_2/CO ratio of DRM production is 1:1 while SRM has a product ratio of 3:1). Additionally, of course, DRM does not require the use of water to produce syn-gas.

Metal carbides are a relatively new family of catalysts for DRM. York et al. [24] studied DRM reactions over β-Mo_2C and WC with a direct comparison with noble metal catalysts. Importantly, the results showed that β-Mo_2C has an activity for DRM comparable to certain noble metals, while the price of molybdenum is much cheaper than noble metals. Furthermore, compared to Ni-based catalysts (arguably the earliest-found material to have a high activity

X. Du · L. J. France · V. L. Kuznetsov · T. Xiao ·
P. P. Edwards (✉)
Inorganic Chemistry Laboratory, Department of Chemistry,
KACST-Oxford Petrochemical Research Centre (KOPRC),
University of Oxford, Oxford OX1 3QR, UK
e-mail: peter.edwards@chem.ox.ac.uk

X. Du
e-mail: xian.du@chem.ox.ac.uk

H. AlMegren · A. Bagabas
Petrochemicals Research Institute (PRI), King Abdulaziz City of
Science and Technology (KACST), P.O. Box 6086, Riyadh
11442, Saudi Arabia

in DRM), Mo_2C, has higher stability due to its enhanced resistance to coking.

The dispersion of catalyst onto a support surface is another critical factor which can significantly influence the catalytic activity of materials [1]. The supported catalyst can play an important role in promoting reaction, which has been proven by many researchers after making a direct comparison between bulk and supported materials on a variety of supports, such as TiO_2, Al_2O_3, SiO_2, and ZrO_2 [3, 12, 19].

In recent years, therefore, supported transition metal carbides have gained increased prominence since the support can improve both the efficiency and the stability of carbides in the DRM reaction. Systematic studies on Mo_2C loaded on different supports have been carried out by Brungs et al. [7] and Darujati et al. [11]. Their results revealed that during a long-term DRM test, when Mo_2C is supported by ZrO_2 and γ-Al_2O_3, the catalytic activity and stability were higher than that for materials loaded on other oxide based supports. The advantage of γ-Al_2O_3 appears to be its significantly higher surface area compared to other kinds of support. But the advantage of ZrO_2 is its amphoteric nature [8]. The Lewis acid sites enhance the dispersion of metal due to the preference of metal atoms to reside at Lewis acid sites on the support [6], whereas the Lewis base sites can enhance the adsorption of CO_2 on the support in conjunction with Lewis acid sites [4]. Moreover, on ZrO_2, it is proposed that CO_2 activation takes place at the interface between carbide and support, which leads to a low oxidation effect on carbides [17].

To-date, the activity and stability of catalysts during DRM reaction have been improved only by a small improvement. Moreover, the product selectivity of catalysts (i.e. specifically the H_2/CO ratio) appeared to differ from a supported catalyst because they have the different activities on CO_2 decomposition and CH_4 cracking and/or the existence of side reactions such as reverse Water–Gas shift ($RWGS, CO_2 + H_2 \rightarrow CO + H_2O, \Delta H_{298}^o = +41$ KJmol^{-1}). Hence, one of the major initiatives for catalyst improvement stem from the need to improve selectivity, by reducing side reactions. Additionally the need to balance the two DRM half reactions, CH_4 cracking and the reverse boudouard reaction, is essential to avoid carbon deposition.

In seeking the high activities (including both the conversion of reactants and the yields of products) and high stabilities, here we prepared the ZrO_2-supported Mo/Co–Mo carbide catalysts for the dry reforming of methane. The incorporation of cobalt into the bimetallic system is because of its high activity in CH_4 decomposition [8] combined with relatively high resistance to coking, when compared to nickel metal [16]. Co–Mo bimetallic carbides have earlier been used for the DRM as an alternative to

expensive noble metal [18], and such Co–Mo bimetallic carbides were systematically prepared and characterized by Xiao et al. [22]. The prepared catalysts were tested under 850 °C, atmospheric pressure and CO_2:CH_4 1:1 conditions for 4 h, and the results not only exhibit the noticeable activity of ZrO_2 support itself but also show the high performance of the novel ZrO_2-supported Co–Mo bimetallic carbide catalyst both in activity and the resistance to deactivation.

Experimental

Catalyst preparation

Zirconia support (Alfa-Aesor, 90 m^2/g) was ground to 64–125 μm and pre-heated at 400 °C (marked as −400), the same temperature as the slurry calcination process. For the purpose of comparison, the same ZrO_2 with the same particle size was pre-heated at 750 °C (marked as −750), the same temperature as the oxide carburization process.

The required amount of ammonium molybdate tetrahydrate (98 %, Sigma Aldrich) and zirconia support were added to distilled water before stirring to generate slurry. The slurry was stirred and heated at 100 °C to remove water prior to calcination in a muffle furnace for 10 h at 400 °C to which the ramping rate was set at 10 °C/min. After the calcination process, the sample of MoO_3/ZrO_2 was obtained.

To obtain the carbide materials, 3.0 g of prepared oxides were carburized in a quartz tube under a gas flow of CH_4/H_2 (8 and 32 ml/min respectively) for 3 h at 750 °C, and both the ramping and cooling rate were 3 °C/min. After carburization, the carbide samples were passivated in static air for 48 h before unloading. The carbide samples were labelled with a percentage of Mo_2C loading in terms of their oxide precursors. All the synthesized catalysts were labeled as X %-Mo-Y (X is the loading of MoO_3 in wt% and Y denotes the pre-heating temperature).

Besides the supported Mo_2C catalysts, the pure ZrO_2 support and the bulk Mo_2C carbide were also prepared from zirconia catalyst support (Alfa-Aesor, 43815, 90 m^2/g) and ammonium molybdate tetrahydrate (98 %, Sigma Aldrich-A7302), respectively via the same method of calcination and carburization processes.

With the aim of preparing Co–Mo bimetallic carbide samples, the required amount of ammonium molybdate tetrahydrate and cobalt(II) nitrate hexahydrate (98 %, Sigma Aldrich) were dissolved in water using the same method as above and the percentage in weight of the bimetallic oxides were 10 and 15 wt% while the Co/Mo ratio was kept at 0.4/0.6 which has been employed

previously and found to possess the highest stability in pyridine hydrodenitrogenation reactions [22].

Catalyst activity test

For catalyst activity and stability tests, materials were placed in an M-R-10A micro-reactor (Kunlun Yongtai Company, China) under temperature-programmed reaction conditions. The catalyst bed was heated in nitrogen gas flow to 600 °C with a 10 °C/min ramping rate and then heated up to 850 °C at 5 °C/min. The gas products were sampled and analysed via online gas chromatography (Shimadzu, GC-2014) every 30 min at 850 °C to test the stability of the catalyst samples. Catalysts were tested under the flow of a calibrated mixed gas that comprised CH_4, CO_2 and N_2 (internal standard). The amount of catalyst was kept at 0.5 g.

With the online GC measurements of outlet gases from the reactor (N_2, CH_4, CO_2, H_2 and CO), the conversions of CH_4 and CO_2, the yields of products (H_2 and CO), and the carbon balance of the reactions can be determined with the following equations:

$$\text{Conversion} = C_i = 1 - \frac{X_i^{\text{outlet}} X_{N_2}^{\text{inlet}}}{X_i^{\text{inlet}} X_{N_2}^{\text{outlet}}} \ (i = CH_4 \text{ or } CO_2)$$

$$\text{Volume of gas in product} = \frac{X_i^{\text{inlet}} \text{ Volume of } N_2}{X_{N_2}^{\text{outlet}}} \ (i = H_2 \text{ or } CO)$$

$$\text{Yield of } H_2 = Y_{H_2} = \frac{\text{volume of } H_2 \text{ in products}}{2 * \text{volume of methane in reactants}}$$

$$\text{Yield of CO} = Y_{CO} = \frac{\text{volume of CO in products}}{\text{volume of } C \text{containing reactants}}$$

$$\text{Product Ratio} = H_2/CO = \frac{\text{volume of } H_2 \text{ in products}}{\text{volume of } CO \text{in products}}$$

$$\text{Carbon Balance} = B_{\text{carbon}} = \frac{(X_{CH_4}^{\text{outlet}} + X_{CO_2}^{\text{outlet}} + X_{CO}^{\text{outlet}})X_{N_2}^{\text{inlet}}}{(X_{CH_4}^{\text{inlet}} + X_{CO_2}^{\text{inlet}})X_{N_2}^{\text{outlet}}}$$

Characterization of catalyst pre- and post- reaction

All the samples, including ZrO_2 support, the various precursors and carbides, were characterized by high-resolution X-ray diffraction (XRD) using a PANalytical X'Pert PRO diffractometer with CuKα radiation (45 kV, 40 mA). The samples were flat loaded in the custom-built sample holders and scanned from 10° to 70° 2θ with a step size of 0.0084° and a scanning speed at 0.017778° s^{-1}.

Raman spectra were collected (resolution of 2 cm^{-1}) using a PerkinElmer Raman Stage 400F with a 785-nm laser. The samples were pressed onto a microscope slide and the scanning time was set to 20 s (repeated 10 times) within the spectral range from 100 to 2,500 cm^{-1}.

Brunauer, Emmett and Teller (BET) analysis via nitrogen adsorption was carried using a Micrometrics Chemi-Sorb 2720 to measure the surface area and pore volume of
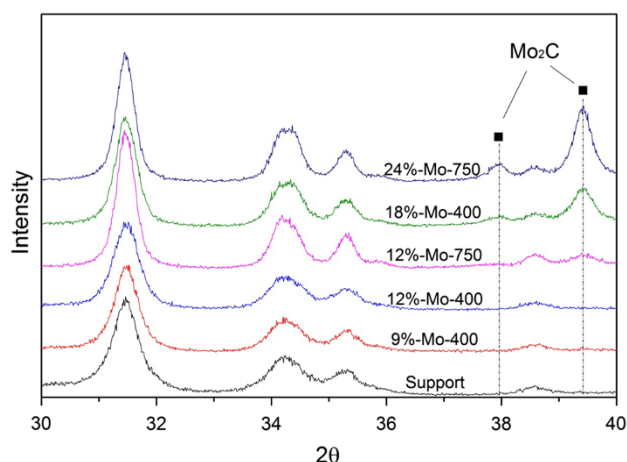

Fig. 1 X-ray diffraction patterns of ZrO_2 supported Mo_2C with different loading level (9–24 wt%) and on ZrO_2 supports with different pre-heating temperature (750 °C, 400 °C, as indicated)

samples both before and after the DRM reactions at the temperature of liquid nitrogen (−195.8 °C).

The carbon deposits of catalysts pre- and post- reaction were measured via thermo-gravimetric analysis (TGA). The instrument employed was a PerkinElmer, TGA-7, using flowing air at 10 ml/min from 50 to 1,000 °C with a ramp rate of 10 °C/min.

Results and discussion

DRM over supported Mo_2C catalysts

Figure 1 shows the XRD patterns of ZrO_2-supported Mo_2C with different loading levels at different pre-heating temperatures. It is apparent that Mo_2C is dispersed differently over the surface of ZrO_2 supports which are pre-heated at 400 and 750 °C, respectively. The peak of Mo_2C at $2\theta = 39.49°$ can be clearly observed on 12 %-Mo-750 carbides while the peaks at the same position can hardly be observed on 12 %-Mo-400, indicating that Mo_2C has a considerably enhanced dispersion on the 400 °C-pre-heated support (this has been shown to have a higher surface area according to Table 2).

In Fig. 2, Laser Raman spectra of Mo_2C 6–24 % loaded on 400 °C-pre-heated ZrO_2 were presented. It was difficult to observe the ZrO_2 support when the loading level was above 12 %, which indicates that the ZrO_2 support had been fully covered by Mo_2C, demonstrating that the availability of the ZrO_2 surface for potential catalytic activation decreased as the loading level increased.

During the process of DRM reaction, CH_4 absorption and subsequent dissociation is usually recognized to be the first step, as well as the rate determining step (1) [13, 20,

21, 23], and this is followed by the oxidation of carbon species (adsorbed carbon and CH_x) on a catalyst surface by CO_2, forming CO (2):

$$CH_4 \leftrightarrow CH_x + (4-x)H \leftrightarrow C + 2H_2 \quad (1)$$

$$CO_2 + C \leftrightarrow 2CO \quad (2)$$
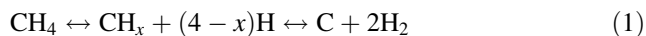
Besides the DRM, a side reaction called "reverse water gas shift" (RWGS, (3)) can lead to a higher conversion of CO_2 and the consumption of generated H_2.

$$H_2 + CO_2 \rightarrow CO + H_2O \quad (3)$$

The activity test results presented in Table 1 show very poor performance of the bulk Mo_2C to activate and convert both CH_4 and CO_2 at atmospheric pressure, and the conversions are even lower than the ZrO_2 support which is "carburized" under the same conditions to prepare carbide catalysts. This can be attributed to the low surface area of the bulk Mo_2C, which leads to a low availability of Mo_2C
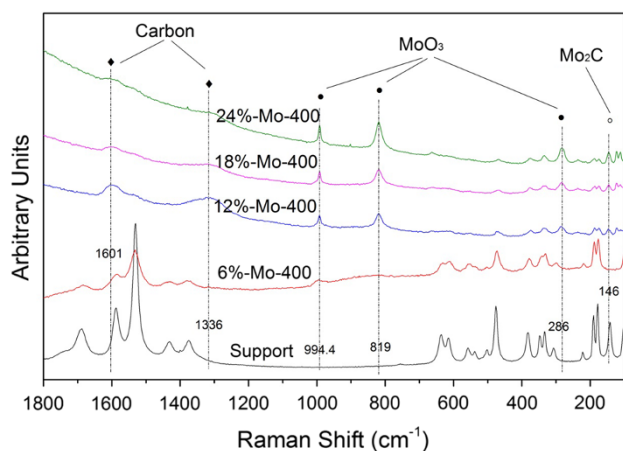

Fig. 2 Laser Raman spectra of Mo_2C 6 %-24 % loaded on 400 °C-pre-heated ZrO_2 (notice: the appearance of MoO_3 in Laser Raman spectra is because the outer layer Mo_2C was oxidized during the passivation step after carburization, and the very thin layer of MoO_3 cannot be observed in the XRD patterns in Fig. 1)

active sites on the surface of material (which is different from the high-surface-area metal carbide materials prepared by Claridge et al. [9].). The activity in converting both CH_4 and CO_2 over pure ZrO_2 support is attributed to its amphoteric property [8]. Both Lewis acid sites and base sites can enhance the adsorption of CH_4 and CO_2 on ZrO_2 surface [4] where the reactants can be activated and converted. According to the product ratio, significantly more CO is generated than H_2, and this is due to the RWGS (reaction (3)).

Importantly, higher activities and stabilities were observed over supported Mo_2C compared to the bulk Mo_2C. Both reactant's conversions and product yields were enhanced due to the Mo_2C dispersion effect, and there is the possibility to attribute this improvement to a synergy between Mo_2C and ZrO_2 support.

Comparison of the catalysts with the same pre-treated supports (400 or 750 °C) revealed that a higher Mo_2C loading level led to a lower conversion of CH_4 and CO_2. This may be due to high levels of Mo_2C dispersed on the surface decreasing the availability of the ZrO_2 support acid sites themselves (shown in Fig. 2, the higher loading level of Mo_2C leads to a lower intensity of ZrO_2 peaks) which as started previously is active for the DMR over its Lewis acid and base sites. Despite the lower CH_4 and CO_2 conversions, the samples with higher loading levels (18 %-Mo-400 and 24 %-Mo-750) also had a similar or slightly higher product yields compared to low loading level. It could be concluded that the higher availability of ZrO_2 surface led not only to a higher conversion but also a higher degree of side reactions (e.g. RWGS) which affected the yields of products.

The catalytic performances over 12 %-Mo-400 and 12 %-Mo-750 (Table 1) were shown to be close to each other at 4 h even though the conversions of CH_4 and CO_2 over 12 %-Mo-400 were higher than the other ones. This phenomenon can be explained by a further sintering effect on the materials when reacting temperature reached to 850 °C, and both catalysts reached the similar Mo_2C

Table 1 Conversion of CH_4 and CO_2, yield of H_2 and CO, product ratio and carbon balance over different samples (bulk Mo_2C, pure ZrO_2 support and ZrO_2 supported Mo_2C catalysts) during DRM reactions (conditions: 850 °C, atmospheric pressure, 4-h duration, CH_4/CO_2 1, GHSV 4.8×10^3 ml h^{-1} g_{cat}^{-1})

Sample	C_{CH_4} (%)		C_{CO_2} (%)		Y_{H_2} (%)		Y_{CO} (%)		H_2/CO		B_{carbon} (%)	
	0 h	4 h	0 h	4 h	0 h	4 h	0 h	4 h	0 h	4 h	0 h	4 h
Bulk-Mo_2C	12.99	14.78	36.89	20.61	7.42	5.65	27.86	19.16	0.26	0.29	106.4	103.8
ZrO_2-support	19.44	23.14	31.35	33.31	8.95	9.38	24.26	25.19	0.35	0.35	98.8	98.2
9 %-Mo-400	41.77	37.56	57.05	52.09	29.17	24.80	43.59	39.39	0.65	0.61	96.6	97.2
12 %-Mo-400	41.46	36.94	56.08	51.50	27.22	22.58	41.03	38.51	0.63	0.57	97.8	98.6
18 %-Mo-400	40.80	36.45	55.09	48.01	31.14	24.47	43.76	38.80	0.66	0.59	97.3	98.0
12 %-Mo-750	40.31	37.42	55.26	51.26	27.82	23.34	40.80	38.28	0.63	0.58	94.9	94.5
24 %-Mo-750	30.93	28.19	46.54	42.85	27.24	23.44	41.99	39.22	0.60	0.55	99.0	99.5

Table 2 Surface area and pore volume of samples (ZrO_2 supported Mo_2C catalysts) pre- and post- reactions

Sample name	Surface area (m^2/g)		Pore volume (cm^3/g)	
	Pre	Post	Pre	Post
9 %-Mo-400	55.77	35.45	0.2612	0.2318
12 %-Mo-750	29.87	24.35	0.2158	0.1624

dispersion level (even though they looked different before the reaction, as shown in Fig. 1).

The carbon balance during reaction over each sample was also displayed in Table 1. It was observed that the carbon balance over Bulk-Mo_2C was above 100 %, revealing that Mo_2C was consumed by CO_2 to form MoO_2 and CO (4). The numbers of carbon balance over ZrO2 support and ZrO2 supported catalysts were slightly below 100 %, which indicates that amorphous carbon was generated during the reaction.

$$Mo_2C + 5CO_2 \rightarrow 2MoO_2 + 6CO \quad (4)$$
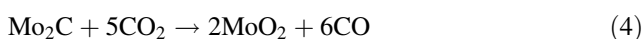
The results of the surface area and pore volume of samples both prior to ("pre-") and post-reaction ("post-") are presented in Table 2. A noticeable difference between the pre-reaction surface areas of the two samples was observed, indicating a more highly sintered ZrO_2 support after being heated at 750 °C.

Moreover, the difference between the post-reaction surface areas of the two samples is much smaller, which is caused by a further sintering effect when the catalyst was heated up to 850 °C during the reaction, and this sintering effect was possibly one of the main routes of deactivation during the dry reforming of methane.

Comparison of the XRD patterns of the supported carbides pre- and post-reaction is presented in Fig. 3. They showed that the MoO_2 peaks at $2\theta = 26.11°$ and $37.12°$ were observed in the post-reaction catalysts. This phenomenon indicated the oxidation of Mo_2C to MoO_2 with CO_2 (4), which is known to be another main deactivation mechanism of DRM [9].

A new peak corresponding to the Mo_2C peak at $2\theta = 39.49°$ was observed. This indicated that Mo_2C crystallized when the surface area of ZrO_2 support decreased during the 4-h activity test (shown in Table 2). The crystallite size of ZrO_2 was also increased as calculated with XRD patterns shown in Fig. 3. (Pre-reaction 340–370 nm; post-reaction 570–630 nm), which is another evidence of minimized sintering effect existing on ZrO_2 support.

In order to elucidate whether the catalysts experienced carbon deposition over the catalysts during the dry reforming of methane, TGA (thermo-gravimetric analysis) was undertaken. Results for the pre- and post- reaction 18 %-Mo-400 catalysts are displayed in Fig. 4 with
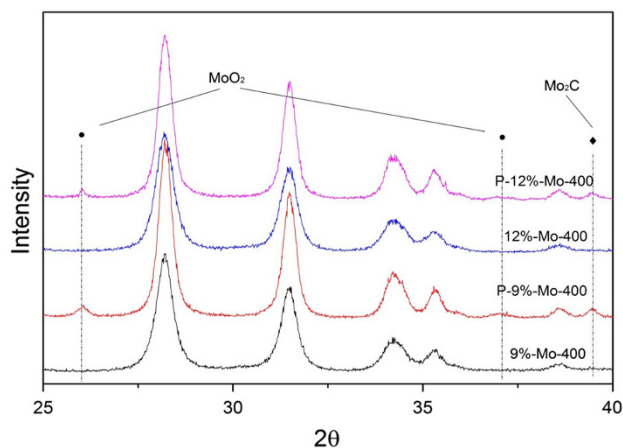
Fig. 3 X-ray diffraction patterns of the ZrO_2 supported Mo_2C catalysts before and after DRM (*P* post-reaction)
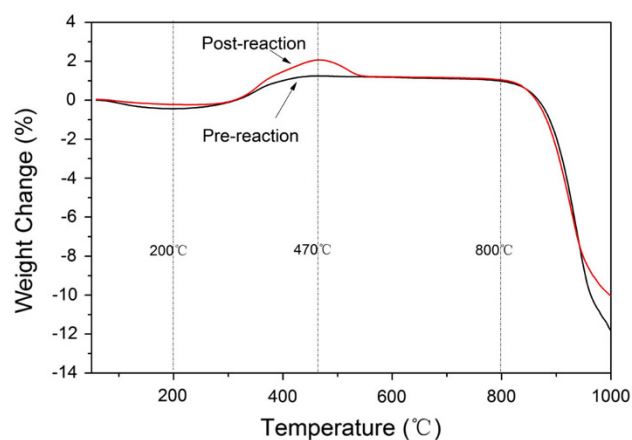
Fig. 4 Thermo-gravimetric analysis of the pre- and post- reaction 18 %-Mo-400 catalysts

Table 3 Weight changes in thermo-gravimetric analysis of the pre- and post- reaction 18 %-Mo-400 catalysts at different temperature ranges

Sample	200–470 °C (%)	470–800 °C (%)	800–1,000 °C (%)
Pre-reaction	1.6784	−0.26314	−13.0005
Post- reaction	2.28482	−1.01721	−11.1111

the calculation of weight change at each temperature range exhibited in Table 3. The weight increased between 200 and 470 °C, which indicated the oxidation of Mo_2C to MoO_3. Weight loss was observed starting at 470 and 800 °C and related to the combustion of amorphous carbon [14] and the sublimation of MoO_3 [15], respectively. The graphitic carbon which is expected to be combusted between 600 and 800 °C [5] can only be observed at an
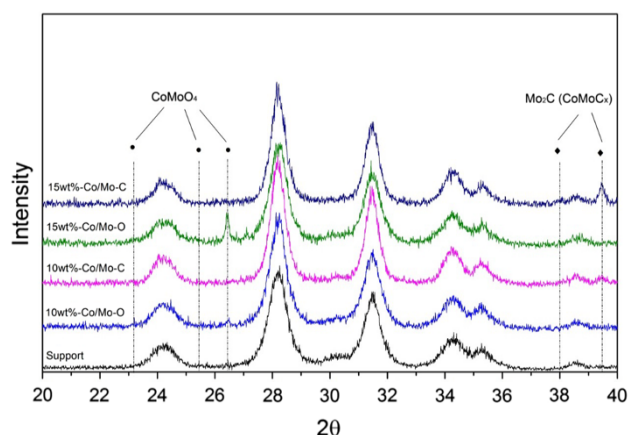
Fig. 5 X-ray diffraction patterns of ZrO_2 supported 10/15 % Co–Mo bimetallic oxides and carbides (*C* carbide, *O* oxide)
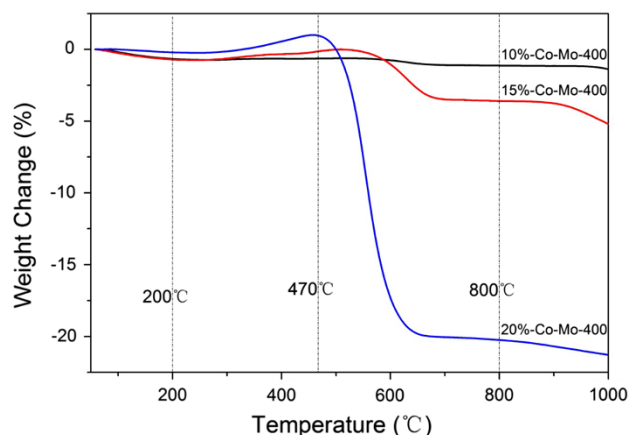

Fig. 6 Thermo-gravimetric analysis of the pre-reaction Co–Mo bimetallic catalysts

Table 4 Weight changes in thermo-gravimetric analysis of pre-reaction Co–Mo bimetallic catalysts at different temperature ranges

Sample	200–470 °C (%)	470–800 °C (%)	800–1,000 °C (%)
10 %-Co–Mo-400	0.0248	−0.495	−0.24795
15 %-Co–Mo-400	0.5874	−3.46087	−1.63518
20 %-Co–Mo-400	1.12482	−21.1706	−1.02829

arguably low level. Upon comparison of these two TGA curves, more amorphous carbon was observed on the post-reaction catalyst, which means the generation of carbon via the decomposition of CH_4 (reaction (1)) occurred on the surface of catalyst during the dry reforming of methane.

DRM on supported Co–Mo carbide catalysts

As an extension of this work based on the results of mono-metallic carbides, bimetallic carbide catalyst systems were also investigated to enhance the activity and stability of catalysts in the dry reforming of methane. The results can be summarized as follows.

In the XRD patterns after incorporating cobalt with the molybdenum catalyst in Fig. 5, the peaks corresponding to the $CoMoO_4$ structure at $2\theta = 23.33°$, $25.50°$ and $26.50°$ were observed. In addition, the Co_3O_4 phase was not observed. This indicated that only $CoMoO_4$ had been formed during the calcination process. After carburisation, phases of Mo_2C at the angle of $2\theta = 38.101°$ and $39.492°$ were observed clearly and there appeared to be no evidence of Co metal particles or Co carbide in the XRD patterns. According to Xiao et al. [22], this phenomenon is attributed to the direct incorporation of cobalt into the lattice of Mo_2C carbide, and due to the comparable atomic radius of Co ($r \approx 126$ pm) compared with that of Mo ($r \approx 154$ pm), the framework of Mo_2C did not change significantly even though the lattice was partially substituted by Co atoms.

The TGA results of the pre-reaction bimetallic catalysts are exhibited in Fig. 6 with the calculation of weight change at each temperature range exhibited in Table 4. From the weight loss observed starting around 470 °C (which is related to the combustion of amorphous carbon), it indicates that the increased loading level of the bimetallic carbide enhanced the formation of carbon during the car-burization step. The weight loss after 800 °C was much
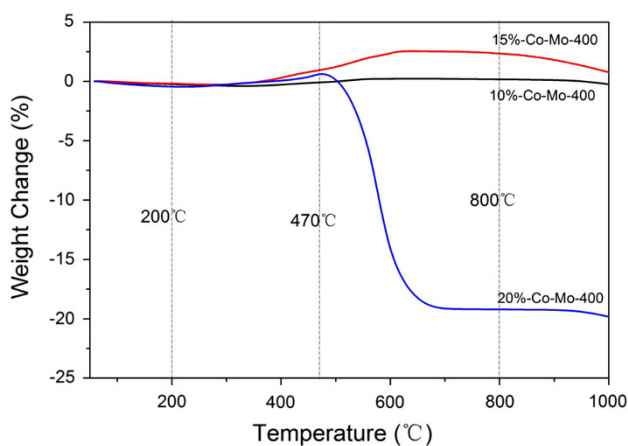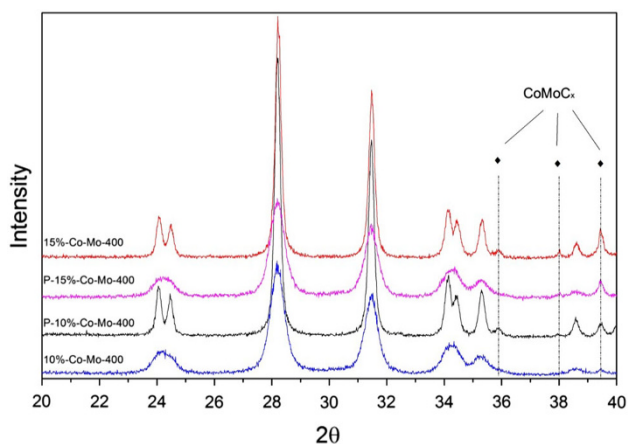
less than that exhibited by the monometallic catalysts (as shown in Fig. 4).

The catalyst activity test results over 10, 15 and 20 % bimetallic carbides are shown in Table 5. With the incorporation of Co into Mo_2C, there was a significant increase in both CH_4 and CO_2 conversion: The conversion of CH_4 was nearly complete and the conversion of CO_2 also reached above 95 % when the loading level of the bimetallic carbide reached 15 % or higher. This very large activity improvement was due to the introduction of Co which has been proven to be very active metal in the DRM reaction. In conjunction with the above, the stabilities of both CH_4 and CO_2 conversions were significantly improved with the addition of Co components. In addition, the stability of both H_2 and CO yields were enhanced as the loading level increased.

The H_2/CO product ratio over all the three bimetallic carbide catalysts (as shown in Table 5) were above 1, which indicated the CH_4 decomposition (reaction 1) was favoured over the bimetallic catalysts. As mentioned in monometallic carbide catalyst discussion, the availability of ZrO_2 contributes to the conversions of both CH_4 and CO_2, and on the other hand, it also improves the side reactions which can lead to the observed difference

Table 5 Conversions of CH_4 and CO_2, yields of H_2 and CO, product ratio and carbon balance over bimetallic carbide samples during DRM reactions (conditions 850 °C, atmospheric pressure, 4 h duration, CH_4/CO_2 1, GHSV 4.8×10^3 ml h^{-1} g$_{cat}^{-1}$)

Sample	C_{CH_4} (%)		C_{CO_2} (%)		Y_{H_2} (%)		Y_{CO} (%)		H_2/CO		B_{carbon} (%)	
	0 h	4 h	0 h	4 h	0 h	4 h	0 h	4 h	0 h	4 h	0 h	4 h
10 %-Co–Mo-400	98.28	97.13	87.04	85.29	94.1	87.9	88.0	82.8	1.13	1.13	98.2	94.4
15 %-Co–Mo-400	97.46	97.46	97.66	95.50	97.9	95.4	89.8	86.2	1.09	1.10	94.2	91.8
20 %-Co–Mo-400	97.75	97.50	98.02	97.07	97.1	95.2	89.8	86.9	1.09	1.09	92.5	92.7

Fig. 7 Thermo-gravimetric analysis of the post-reaction Co–Mo bimetallic catalysts

Fig. 8 X-ray diffraction patterns of ZrO_2 supported 10/15 % Co–Mo bimetallic carbides before and after the dry reforming of methane (*P* post-reaction)

Table 6 Weight changes in thermo-gravimetric analysis of pre-reaction Co–Mo bimetallic catalysts at different temperature ranges

Sample	200–470 °C (%)	470–800 °C (%)	800–1,000 °C (%)
10 %-Co–Mo-400	0.15786	0.25653	−0.40511
15 %-Co–Mo-400	1.15481	1.37135	−1.60592
20 %-Co–Mo-400	1.05181	−19.8175	−0.60463

The TGA results of the post-reaction bimetallic catalysts are exhibited in Fig. 7 with the calculation of weight change at each temperature range exhibited in Table 6. No weight losses are observed on 10 %-Co–Mo-400 and 15 %-Co–Mo-400, and arguably, there is a reduction of weight loss from 470 °C on 20 %-Co–Mo-400 (the gain of weight from 200 °C over 20 %-Co–Mo-400 is masked by the great weight loss from 470 °C, which means the carbon hasn't been totally consumed during DRM). This phenomenon on bimetallic catalysts indicated the consumption of carbon by CO_2 ($CO_2 + C \leftrightarrow 2CO$, reaction (3)) during the dry reforming of methane, favouring to the CO production. However, the carbon balances of reaction over bimetallic catalysts (Table 5) were below 100 %, which indicates that carbon-containing product apart from CO and coke was generated during the reaction, and the unexpected product is hypothesized as light hydrocarbons.

The very high stabilities of Co–Mo bimetallic carbide catalysts were also exhibited in their XRD patterns after being tested in the dry reforming of methane. In Fig. 8, only the peaks corresponding to $CoMoC_x$ were observed on the ZrO_2 support and there appeared to be no evidence of MoO_2 or $CoMoO_x$ generation. Compared to the formation of MoO_2 over ZrO_2 supported Mo_2C catalysts (shown in Fig. 3), these catalysts exhibited significantly enhanced oxidation resistance as the bi-metallic carbide phase, this could be explained by the presence of cobalt in the carbide, which may directly enhance the oxidative resistance of the carbide, or provide a re-carburisation route for the oxidized molybdenum (Table 6).

between the conversions and the product yields. As exhibited in Table 5, the conversions of CH_4 and the yields of H_2 were arguably at the same level. This phenomenon indicated that the incorporation of Co into the Mo_2C catalysts can significantly depress the Reverse Water Gas Shift (reaction (3)).

Conclusions

These investigations have shown that bulk Mo_2C did not exhibit a significantly high activity in the dry reforming of methane (DRM); this was attributed to the very low surface area when using the preparation method as described. On the other hand, pure ZrO_2 support was treated with the same method to give ZrO_2 supported Mo_2C catalyst, and this exhibited a relatively higher activity compared to the bulk Mo_2C. It appeared that Lewis acid and base sites on the support ZrO_2 had contributed to this enhanced activity.

The catalytic activity decreased slightly with time on stream for the supported Mo_2C over a period of 4 h. It was thought that this deactivation was caused by two effects: one was the oxidation effect on Mo_2C by CO_2, and the other one was the loss of surface area caused by sintering effect of the ZrO_2 support.

ZrO_2 supported cobalt and molybdenum bi-metallic carbide catalysts were also prepared and examined for catalytic activity. Significant enhancements were observed for both the activity and the stability of the catalysts in the DRM. It was observed also that the incorporation of cobalt atoms into the Mo_2C lattice significantly improved the materials' resistance to aerial oxidation. Compared to the mono-metallic carbide, the bi-metallic catalysts clearly have significantly higher CH_4 conversion. Moreover, an increase of Co loading in the mixed carbide also reduced the influence of Reverse Water Gas Shift, which improved the stability of H_2 yields.

References

1. Al-Fatesh ASA, Fakeeha AH (2011) Reduction of green house gases by dry reforming: effect of support. Res J Chem Environ 15(2):259–268
2. Ashcroft AT, Cheetham AK, Green MLH, Vernon PDF (1991) Partial oxidation of methane to synthesis gas using carbon dioxide. Nature (London) 352(6332):225–226
3. Basini L, Sanfilippo D (1995) Molecular aspects in syn-gas production: the CO2-reforming reaction case. J Catal 157(1):162–178
4. Bhattacharyya K, Danon A, Vijayan BK, Gray KA, Stair PC, Weitz E (2013) Role of the surface lewis acid and base sites in the adsorption of CO_2 on titania nanotubes and platinized titania nanotubes: an in situ FT-IR study. J Phys Chem C 117(24):12661–12678
5. Bom D, Andrews R, Jacques D, Anthony J, Chen B, Meier MS, Selegue JP (2002) Thermogravimetric analysis of the oxidation of multiwalled carbon nanotubes: evidence for the role of defect sites in carbon nanotube chemistry. Nano Lett 2(6):615–619
6. Bradford MCJ, Vannice MA, Ruckenstein E (1999) CO_2 reforming of CH_4. Catal Rev Sci Eng 41(1):1–42
7. Brungs AJ, York APE, Claridge JB, Marquez-Alvarez C, Green MLH (2000) Dry reforming of methane to synthesis gas over supported molybdenum carbide catalysts. Catal Lett 70(34):117–122
8. Budiman AW, Song S-H, Chang T-S, Shin C-H, Choi M-J (2012) Dry reforming of methane over cobalt catalysts: a literature review of catalyst development. Catal Surv Asia 16(4):183–197
9. Claridge JB, York APE, Brungs AJ, Marquez-Alvarez C, Sloan J, Tsang SC, Green MLH (1998) New catalysts for the conversion of methane to synthesis gas: molybdenum and tungsten carbide. J Catal 180(1):85–100
10. Courty P, Durand D, Freund E, Sugier A (1982) C1-C6 alcohols from synthesis gas on copper-cobalt catalysts. J Mol Catal 17(2–3):241–254
11. Darujati ARS, Thomson WJ (2005) Stability of supported and promoted-molybdenum carbide catalysts in dry-methane reforming. Appl Catal A 296(2):139–147
12. Erdoehelyi A, Cserenyi J, Papp E, Solymosi F (1994) Catalytic reaction of methane with carbon dioxide over supported palladium. Appl Catal A 108(2):205–219
13. Erdohelyi A, Cserenyi J, Solymosi F (1993) Activation of methane and its reaction with carbon dioxide over supported rhodium catalysts. J Catal 141(1):287–299
14. Fakeeha AH, Khan WU, Al-Fatesh AS, Abasaeed AE (2013) Stabilities of zeolite-supported Ni catalysts for dry reforming of methane. Cuihua Xuebao 34(4):764–768
15. Halawy SA, Mohamed MA, Bond GC (1993) Characterization of unsupported molybdenum oxide-cobalt oxide catalysts. J Chem Technol Biotechnol 58(3):237–245
16. Luisetto I, Tuti S, Di Bartolomeo E (2012) Co and Ni supported on CeO_2 as selective bimetallic catalyst for dry reforming of methane. Int J Hydrogen Energy 37(21):15992–15999
17. Naito S, Tsuji M, Miyao T (2002) Mechanistic difference of the CO_2 reforming of CH_4 over unsupported and zirconia- supported molybdenum carbide catalysts. Catal Today 77(3):161–165
18. Shao H, Kugler EL, Ma W, Dadyburjor DB (2005) Effect of temperature on structure and performance of in-house cobalt-tungsten carbide catalyst for dry reforming of methane. Ind Eng Chem Res 44(14):4914–4921
19. Steinhauer B, Kasireddy MR, Radnik J, Martin A (2009) Development of Ni–Pd bimetallic catalysts for the utilization of carbon dioxide and methane by dry reforming. Appl Catal A 366(2):333–341
20. Takayasu O, Hongo N, Matsuura I (1993) Spillover effect for the reducing reaction of CO_2 with CH_4 over SiO_2-supported transition-metal catalysts physically mixed with MgO. Stud Surf Sci Catal 77:305–308
21. Tsipouriari VA, Zhang Z, Verykios XE (1998) Catalytic partial oxidation of methane to synthesis gas over Ni-based catalysts I. Catalyst performance characteristics. J Catal 179(1):283–291
22. Xiao T-C, York APE, Al-Megren H, Williams CV, Wang H-T, Green MLH (2001) Preparation and characterization of bimetallic cobalt and molybdenum carbides. J Catal 202(1):100–109
23. Yan Z-F, Ding R-G, Song L-H, Qian L (1998) Mechanistic study of carbon dioxide reforming with methane over supported nickel catalysts. Energy Fuels 12(6):1114–1120
24. York APE, Claridge JB, Brungs AJ, Tsang SC, Green MLH (1997) Molybdenum and tungsten carbides as catalysts for the conversion of methane ot synthesis gas using stoichiometric feedstocks. Chem Commun (Cambridge) 1:39–40